Physical and Engineering Sciences in Medicine (2023) 46:575–583
https://doi.org/10.1007/s13246-023-01233-8

SCIENTIFIC PAPER

An anthropomorphic 3D printed inhomogeneity thorax phantom slab for SBRT commissioning and quality assurance

Stephen How[1] · Dilli Banjade[1] · Scott Crowe[2] · Greg Dillon[1] · Andrew Skimmings[3]

Received: 10 July 2022 / Accepted: 9 February 2023 / Published online: 20 February 2023

Abstract

Anthropomorphic phantoms with tissue equivalency are required in radiotherapy for quality assurance of imaging and dosimetric processes used in radiotherapy treatments. Commercial phantoms are expensive and provide limited approximation to patient geometry and tissue equivalency. In this study, a 5 cm thick anthropomorphic thoracic slab phantom was designed and 3D printed using models exported from a CT dataset to demonstrate the feasibility of manufacturing anthropomorphic 3D printed phantoms onsite in a clinical radiotherapy department. The 3D printed phantom was manufactured with polylactic acid with an in-fill density of 80% to simulate tissue density and 26% to simulate lung density. A common radio-opacifier, barium sulfate ($BaSO_4$), was added 6% w/w to an epoxy resin mixture to simulate similar HU numbers for bone equivalency. A half-cylindrical shape was cropped away from the spine region to allow insertion of the bone equivalent mixture. Two Gafchromic™ EBT3 film strips were inserted into the 3D printed phantom to measure the delivery of two stereotactic radiotherapy plans targeting lung and bone lesions respectively. Results were analysed within SNC Patient with a low dose threshold of 10% and a gamma criterion of 3%/2 mm and 5%/1 mm. The resulting gamma pass rate across both criterions for lung and bone were ≥ 95% and approximately 85% respectively. Results shows that a cost-effective anthropomorphic 3D printed phantom with realistic heterogeneity simulation can be fabricated in departments with access a suitable 3D printer, which can be used for performing commissioning and quality assurance for stereotactic type radiotherapy to lesions in the presence of heterogeneity.

Keywords 3D printing · Inhomogeneity · Phantom · SBRT · Commissioning · Quality assurance

Introduction

Additive manufacturing, also known by its colloquial term 3D printing, has demonstrated the possibility of manufacturing geometrically accurate, tissue representative phantoms for a wide variety of applications in the medical sciences such as the field of radiation therapy. There has been much interest in the area of manufacturing phantoms that increasingly approximates realistic patient geometry and tissue equivalency [1–7]. An application of a 3D printed phantom is for stereotactic body radiotherapy (SBRT) which has a number of additional challenges to consider for quality assurance. SBRT is a higher complexity radiotherapy treatment typified by high dose per fraction, multi-leaf collimator (MLC) defined small fields, and a requirement for sub-millimetre accuracy [8]. SBRT is a now a widely accepted treatment modality on C-arm linear accelerators (LINAC) for treating small lesions in the presence of tissue heterogeneity such as lung and bone.

The American Association of Physicists in Medicine (AAPM) Task Group 101 report recommends that the cumulative system uncertainty for the SBRT process be quantified through an end-to-end test [9]. Some traditional treatment planning system (TPS) dose calculation algorithms have historically performed worse in the presence of small field heterogeneities [10, 11]. This uncertainty should be quantified through an end-to-end test on a suitable phantom, however current commercial phantoms consist mainly of simple geometrical shapes made up of solid water equivalent material.

✉ Stephen How
Stephen.How@health.nsw.gov.au

1 Central West Cancer Care Centre, 1503 Forest Rd, Orange, NSW 2800, Australia

2 Royal Brisbane and Women's Hospital, Butterfield St, Herston, QLD 4029, Australia

3 North West Cancer Centre, Dean St, North Tamworth, NSW 2340, Australia

As a result, dose modelling in the presence of heterogeneities for small-fields is not as robustly tested with traditional commercial phantoms.

To fill this gap, 3D printing allows fabrication of customisable 3D printed phantoms that can sufficiently meet this requirement for quality assurance of SBRT type treatments [12, 13]. The base anthropomorphic phantom structure contours can be exported as a 3D object (.stl file) from a CT dataset of a phantom or patient and then imported into a 3D modelling program such as TinkerCad (Autodesk, USA) for editing. The object file is edited within the modelling program allowing for the insertion of dosimeters for commissioning and quality assurance measurements. This in turn will be exported to a slicing program such as Ultimaker Cura (Ultimaker, Netherlands) which modifies the in-fill densities and converts to a .gcode file which contains the machine instructions for 3D printing.

Thermoplastic filaments such as polylactic acid (PLA) or acrylonitrile butadiene styrene (ABS) at a high in-fill density (typically 80–90% in-fill) have demonstrated excellent dosimetric properties for near tissue equivalence [14, 15]. Tissue equivalent structures are often extruded using a small nozzle (0.4 mm diameter) which offers a good balance between printing speed, resolution and geometrical accuracy. Tino et al. [16] has also described a method to reproduce suitable lung equivalency by using gyroid structures at lower in-fill densities (typically 20–30% in-fill PLA) which has been replicated in other works [17, 18]. However, substitutes 3D printed for bone equivalency have been more difficult to fabricate in comparison. There are two main methods to substitute for higher density tissues. These include 3D printing using higher density thermoplastic filaments or printing the moulds with normal filaments which are then filled with a resin mixed with radio-opacifiers [19].

Works by Okkalidis et al. [2] and Kairn et al. [20] have demonstrated the feasibility of combining 50% gravimetrically measured powdered stone commercial filaments with 50% PLA thermoplastic filament for the replication of bone equivalent density. This allows for the 3D printing of geometrically accurate structures with superior bone radiological equivalence than using resins mixed with radio-opacifiers. However this approach must be performed with a larger nozzle ($\geq$0.6 mm) due to concerns of abrasion and wear on the nozzle when using higher density filaments which offsets some of the geometrical accuracy which can be gained with 3D printing using higher density filaments [20]. Additionally, it is recommended that a dual nozzle printer be used for simultaneous 3D printing of tissue and bone. That in combination with the cost of accessing these specialist thermoplastic filament types can incur a significantly increased expense for clinical departments.

A cost-effective alternative would be to 3D print a mould of the bone structure and then to pour in an equivalent bone density substitute into the mould [19]. The advantage of this method is that the raw materials are readily available and inexpensive for clinical departments. Common contrast-agents such as Barium Sulfate ($BaSO_4$) are used for diagnostic or therapeutic purposes and should be readily available as a radio-opacifier. A method for controlling the HU number can be performed by adding different amounts of radio-opacifier into a potting mixture of epoxy resin. The disadvantage is that trapped air bubbles and expansion/contraction during its setting will result in losing geometrical accuracy which may require further post processing. In addition, Crowe et al. [21] has shown that radio-opacifiers with radiological properties that were measured in the kilo-voltage (kV) energies on a CT scanner may not strictly translate over to megavoltage (MV) energies on a MV LINAC.

The aim of this study was to demonstrate the feasibility of fabricating a thoracic anthropomorphic phantom slab with realistic tissue equivalent densities 3D printed using a novel approach. The potential uses for this custom-designed phantom in the quality assurance of complex treatment techniques such as SBRT delivered by megavoltage C-arm LINACs was then investigated. This was achieved by designing a 3D printed phantom using models exported from a thorax CT dataset, and then fabricated with tissue, lung and bone equivalent 3D printing substitutes for realistic heterogeneity simulation.

Methods

Tissue equivalency characterisation

The 3D printer used in this project was an Ultimaker S5 (Ultimaker, Netherlands). It is a dual nozzle printer which relies on the Material Extrusion (MEX) technique to print by depositing the thermoplastic filament layer by layer [5]. The dual nozzle allows the 3D printer to perform dual-material printing including water-soluble support structures which are required when printing objects with large overhangs or gaps. The thermoplastic filament used was 2.85 mm PLA purchased from RS PRO (RS Components Pty Ltd, mass density: 1.24 g/cm^3), which extrudes through a nozzle diameter of 0.4 mm at a temperature of 230 °C. A higher temperature than the common 190–215 °C was required to reduce the effects of stringing or poor bonding from a higher filament throughput based on experiences using the maximum printer speed setting. The maximum build plate volume on the Ultimaker S5 in the XYZ directions is 330 × 240 × 300 mm^3 and the build plate temperature was set to 60 °C.

The method to characterise tissue equivalency of the 3D printed substitutes was adapted from Dancewicz et al. [22]. Test inserts for tissue, lung and bone which exactly matched the insert dimensions for the Gammex 467 RMI phantom

(Gammex Inc., USA) were 3D printed (Fig. 1a). Then, they were inserted into the RMI phantom and scanned with a Siemens SOMATOM go.Open Pro (Siemens Healthineers AG, Germany) CT scanner using the departmental clinical chest protocol (120 kVp and 2 mm slice thickness). A number of 3D printed inserts were measured at once in the RMI phantom with individual varying physical density (Fig. 1b). The electron density relative to water (RED_w) of each insert were then compared to the equivalent commercial inserts to determine the 3D printed substitute that best resembled the tissue, lung and bone.

The mean HU number was extracted from the CT scan dataset using an ROI tool (1 cm × 1 cm area) in the Eclipse TPS (Varian Medical Systems, USA). 3D printed tissue inserts were fabricated with zig-zag in-fill densities ranging from 80 to 100% while lung inserts had gyroid in-fill densities ranging from 5 to 30%. The zig-zag in-fill structure was chosen for tissue equivalency to reduce the appearance of tiny air gaps in an otherwise full solid which can show a noticeable lower mass density by up to − 7%. The gyroid structure was chosen for lung equivalency to simulate the changes in density in normal lung tissue. The target HU numbers for tissue equivalent density was 0 HU and for lung equivalent density was around − 650 HUs.

The bone equivalent material involved mixing X-OPAQUE-HD Barium Sulfate Suspension Formulation (ATX Medical Solutions) with an epoxy resin potting mix (RS Components Pty Ltd) at various percentage by weight (% w/w). The epoxy resin by itself is close to tissue equivalent density and was created using a two part potting mix with epoxy resin added to a hardener in a 1:1 ratio before allowing to set. The reaction of the epoxy resin with hardener is exothermic, so care was taken to ensure that the heat produced did not significantly warp the 3D printing mould. In the initial hour post-mixing, the potting mixture was stirred thoroughly to reduce the amount of higher density $BaSO_4$ settling towards the bottom of the mould. The % w/w of $BaSO_4$ was varied from 2 to 10% relative to the epoxy resin potting mix. The target HU number for bone equivalent density was around 700 HU but adding different amounts of $BaSO_4$ can produce radiological equivalency for other densities of bone such as cancellous bone (approx. 300 HUs) or cortical bone (approx. 1250 HUs).

TPS vs film percentage depth dose (PDD)

In order to characterise the dosimetric impact of the fabricated 3D printed substitutes for lung and bone, the percentage depth dose (PDD) was measured with Gafchromic™ EBT3 film inserted along the central axis positioned between two solid water phantoms (Fig. 2). Individual 3D printed phantom slabs of 5 cm lung slab and 2 cm bone slab were placed on top of 8 cm solid water and CT scanned using the same scanner and clinical protocol as mentioned previously. A treatment plan was created on the CT dataset in the Varian Eclipse v16.1 TPS using the AcurosXB dose calculation algorithm (Varian Medical Systems, USA). The treatment plan consisted of a 6 MV-stereotactic radiosurgery (SRS) beam and 10 × 10 cm^2 field size with the isocentre located at a source-to-axis distance (SAD) of 100 cm to the surface of the solid water. The 6 MV-SRS beam utilizes a smaller flattening filter than conventional beams in order to achieve a higher maximum dose rate of 1000 MU/min. The plan was then delivered on a Varian C-Series Trilogy LINAC with lung and bone slabs positioned atop the solid water phantom. The measured film PDD was then plotted against the central axis depth dose on the TPS for both lung and bone tissue types.

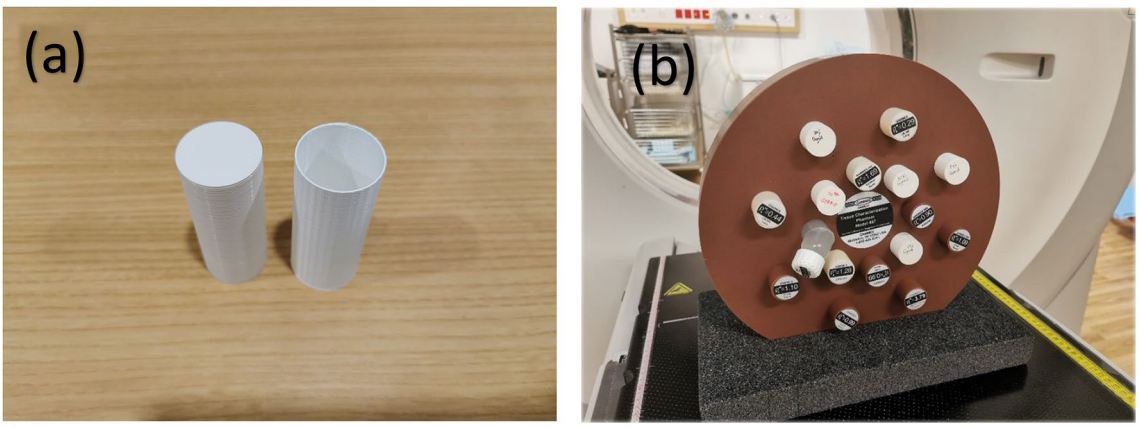

Fig. 1 **a** 3D printed inserts and moulds for inserting into the Gammex 467 RMI phantom **b** Gammex 467 RMI phantom for characterising the RED_w

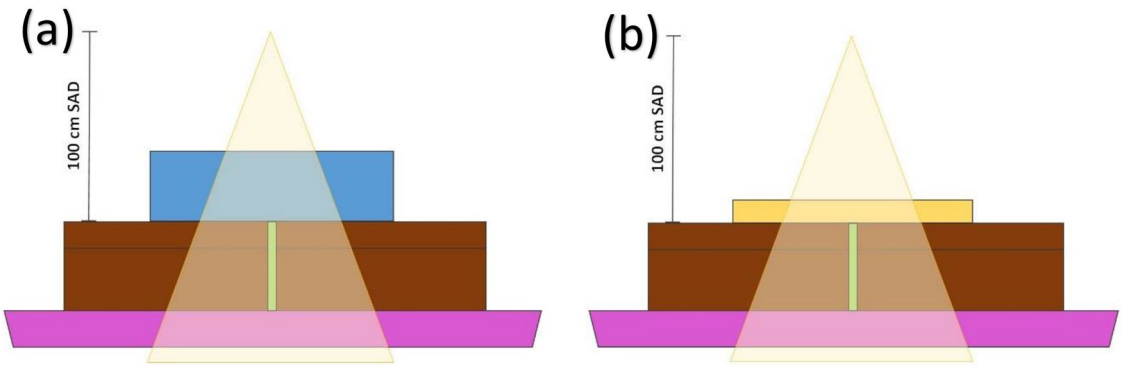

Fig. 2 Setup used for measuring depth doses with the **a** 5 cm lung slab (blue) and **b** 2 cm bone slab (yellow) placed on top of an 8 cm solid water phantom (brown) with film (green) positioned between them. Figure is not to scale

Anthropomorphic 3D printed phantom

To fabricate the anthropomorphic phantom, an anonymized CT dataset of a patient previously treated with lung SBRT was imported into the TPS contouring workspace. Written informed consent was obtained to use the de-identified CT dataset as a quality improvement activity with approval from the Greater Western Human Research Ethics Committee (2022/ETH01181) in accordance with the National Statement on Human Conduct in Research 2007 (updated 2018) [23].

The body and lung structures were contoured for a 5 cm thick section of the patient. The contours were then exported as structures in 3D object files (.stl) into an online computer aided design (CAD) software TinkerCAD (Autodesk, USA). The lung structure was placed at the correct anatomical position with respect to the body structure and a half cylinder was cropped from the spine region to form a simplistic mould for the bone equivalent substitute. Due to the size constraints on the 3D printer build volume, half the body contour was cropped in the sagittal direction and the resulting model had to be additionally shrunk by 50%. Two 15 mm wide × 1 mm high strips were also cropped through the phantom and added to the bone mould to allow the insertions of strips of Gafchromic™ EBT3 radiochromic film through the lung and bone regions.

The modified phantom 3D object file was then exported into Ultimaker Cura 4.6 (Ultimaker, Netherlands) where the in-fill densities were input and the file was converted into .gcode machine instructions for the 3D printer. The body was set to PLA 80% zig zag in-fill for tissue equivalency while the lung was set to PLA 26% gyroid in-fill for lung equivalency. An in-fill density of 80% was chosen for tissue as it was more convenient on printing times and cost-efficient while still remaining close to tissue equivalency. The phantom, which was half of a patient's body contour had a mass of 1.414 kg, with an estimated cost of $154.29 AUD and 3 days, 5.5 h to 3D print. Once completed, the 6% w/w $BaSO_4$ epoxy resin mixture was added to the bone mould and allowed to set overnight to simulate a half-cylindrical spine. The strips through the phantom were removed of any debris to allow radiochromic film strips to fit comfortably through the phantom.

End-to-end test with Gafchromic™ EBT3 film

The 3D printed phantom CT scan was imported into the Eclipse TPS and verification plans were created for SBRT treatments from previous patients, targeting lung and bone respectively. The location of the isocentre was adjusted such that a lung SBRT plan had its isocentre placed in a lung region while a bone SBRT plan had its isocentre placed in the spine region. The coronal dose plane at the location of the isocentre was exported from the TPS into SNC Patient 8.4.1.2 (Sun Nuclear Corporation, Japan) where it was used for comparison with Gafchromic™ EBT3 film.

Strips of 1.4 cm wide Gafchromic™ EBT3 film were inserted into the 3D printed phantom through the isocentre of each plan and the SBRT treatment plans were delivered on a Varian Trilogy C-Series machine with the 6 MV-SRS energy. After delivery, the film was handled as per the film handling protocol based on Lewis et al. [24]. The film was left for 1 h after exposure before scanning on an EPSON Expression 10000XL flatbed scanner (EPSON, Japan). The film was scanned with a resolution of 75 dpi, no colour correction, and a consistent orientation to the calibration film. The resulting 48-bit TIFF film image was then imported into SNC Patient for analysis.

The imported film measurements were manually registered with the coronal dose plane and then analysed using global normalization with a 10% threshold and a gamma criteria of 3%/2 mm or 5%/1 mm. Registration of the film with the TPS dose plane was difficult due to the small film area used (1.4 cm wide strip). Registration was done by manually

matching the absolute isodose lines as close as possible to each other for maximum agreement. Due to delamination uncertainties, results 1 mm from the film edge were cropped to reduce uncertainty in the results.

Results

Tissue equivalency characterisation

Table 1 shows the RED_w for the various 3D printed inserts that were tested. The RED_w was measured using the aforementioned Siemens SOMATOM go.Open Pro CT scanner with the clinical chest protocol (120 kVp, 2 mm slice thickness). The final product was designed to have electron densities as close as possible to their commercial tissue counterparts (Table 2 Electron densities for a subset of Gammex 467 RMI commercial inserts as well as mean HU numbers as measured using the same CT scanner and clinical protocol (120 kVp, 2 mm slice thickness)) for realistic tissue equivalent simulation. Inserts for lung and bone showed that approximately 25–30% gyroid in-fill density was suitable for a 3D printed lung substitute and approximately 6% w/w of $BaSO_4$ added to an epoxy potting mix was suitable for a 3D printed bone substitute. The mean HU numbers of the commercial inserts were within the uncertainty interval of mean HU values for the 3D printed inserts.

TPS vs film percentage depth dose (PDD)

The TPS vs Film PDDs in the solid water phantom are shown in Fig. 3 for lung and bone respectively. A uniform red band uncertainty interval of ± 3% is drawn around the Film PDD (red) for comparison. The TPS depth dose shows satisfactory agreement with the measured film PDD at depths especially after the build-up region (~ 1.3 cm depth).

Table 2 Electron densities for a subset of Gammex 467 RMI commercial inserts as well as mean HU numbers as measured using the same CT scanner and clinical protocol (120 kVp, 2 mm slice thickness)

Commercial insert	$RED_w(\rho_e/\rho_{e,w})$	Mean HU number (HU)
LN-300 Lung	0.282	− 720
LN-450 Lung	0.430	− 550
Solid Water	0.988	+ 10
CB2—30% $CaCO_3$	1.277	+ 460
CB2—50% $CaCO_3$	1.470	+ 830

Anthropomorphic 3D printed phantom

The anthropomorphic 3D printed phantom (Fig. 4) RED_w, mean HU number and standard deviation (k = 2) as measured with a 1 cm × 1 cm square ROI tool are shown in Table 3. The mean HU numbers for the phantom were within the uncertainty of our target inserts for tissue (0 HU), lung (− 650 HU) and bone (700 HU) equivalency. There was a similar standard deviation for both tissue, lung and a better uniformity for the bone substitute in the phantom compared to the inserts. This is attributed to an easier time of mixing the higher density $BaSO_4$ due to a smaller 3D printed mould.

End-to-end test with Gafchromic™ EBT3 film

The gamma pass rates are shown in Table 4 for both 5%/1 mm and 3%/2 mm. The gamma pass rate for lung was ≥ 95% while the gamma pass rate for bone was ~ 85%.

Table 1 Table of 3D printed test inserts electron densities relative to water, mean HU number and standard deviation (k = 2) as measured using the same CT scanner and clinical protocol (120 kVp, 2 mm slice thickness)

3DP material substitute	$RED_w(\rho_e/\rho_{e,w})$	Mean CT number (HU)	± SD (HU)
PLA 5% gyroid in-fill	0.099	− 930	40
PLA 10% gyroid in-fill	0.145	− 875	30
PLA 20% gyroid in-fill	0.227	− 775	30
PLA 25% gyroid in-fill	0.290	− 700	30
PLA 30% gyroid in-fill	0.335	− 645	20
PLA 80% zig-zag in-fill	0.987	− 15	20
PLA 90% zig-zag in-fill	0.990	0	20
PLA 100% zig-zag in-fill	1.081	160	10
Approx. 2% w/w $BaSO_4$ in epoxy resin	1.157	300	200
Approx. 4% w/w $BaSO_4$ in epoxy resin	1.231	400	160
Approx. 6% w/w $BaSO_4$ in epoxy resin	1.402	700	180
Approx. 8% w/w $BaSO_4$ in epoxy resin	1.480	850	100
Approx. 10% w/w $BaSO_4$ in epoxy resin	1.560	1000	100

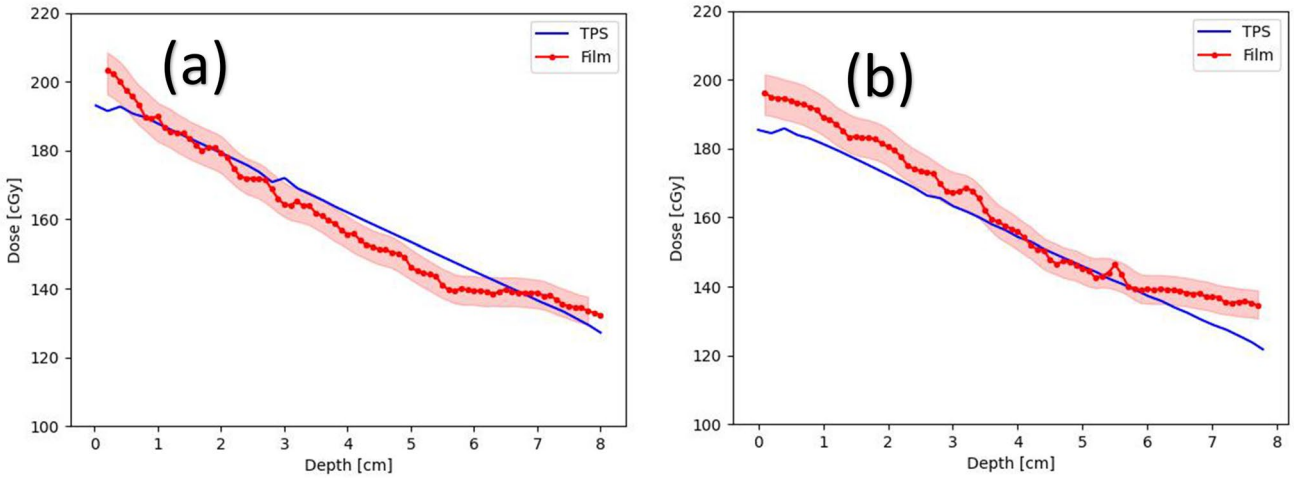

Fig. 3 The measured film PDD vs the TPS central axis depth dose with a red band of smoothed uniform ± 3% uncertainty plotted for the setup using the 3D printed **a** lung and **b** bone slab, respectively

The lower gamma pass rate in the bone SBRT plan were due to the edge of the phantom being at a spine-air interface. The lack of backscatter and charged particle equilibrium (CPE) conditions resulted in the TPS overestimating the dose that would be measured by the film in the spine region.

Discussion

The RED_w of the 3D printed equivalent substitutes matched within uncertainty of equivalent commercial inserts. Additionally, the dosimetric impact of lung and bone substitutes was characterised using PDD comparisons between measured film and the Eclipse TPS. Lung and bone equivalent 3D printed slabs were placed atop of solid water with Gafchromic™ EBT3 film positioned along the central axis. It was found that there was agreement between the measured Film and modelled TPS depth dose. However, in the build-up region (~ 1.3 cm depth) where there is a lack of charged particle equilibrium (CPE), the TPS will underestimate the dose compared to film PDD measurement.

The ideal method to simulate bone equivalent density is to use higher-density thermoplastic filaments such as gravimetrically measured powdered stone mixed into the thermoplastic PLA filament. The advantage is the better geometrical accuracy/uniformity in the 3D printed object and the ease of using different in-fill densities to simulate different bone densities. However, 3D printing with higher-density thermoplastic filaments requires the use of a dual nozzle printer and there are challenges with the increased abrasion to the 3D printer nozzle. Additionally higher-density thermoplastic filaments can be less cost-effective than radio-opacifiers which are readily available in clinical departments.

The production of a 3D printed phantom is limited by the build volume of the 3D printer, thermal warping of large prints, and the cost of the thermoplastic filament. Joining separate 3D printed slabs together will allow the fabrication of larger sized anthropomorphic phantoms that could fully replicate a patient's geometry. Larger phantoms would provide full scatter conditions, allowing larger pieces of radiochromic film to be used for measurement, and providing additional dosimetry data for comparison against TPS dose calculations.

For end-to-end testing, two SBRT plans with isocentres set in the lung and bone region respectively were delivered to Gafchromic™ EBT3 film strips inserted through the 3D printed phantom. The gamma pass rate result for lung was ≥ 95% and the gamma pass rate result for bone was approximately 85%. These results are reasonably consistent with results reported for a 3D-printed customisable anthropomorphic thoracic phantom slab by Tino et al. [1] who reported a pass rate of 98.9% and 90.25% in lung and bone respectively for a 5%/1 mm gamma analysis criterion using film. This reduced gamma pass rate reported in this study is likely due to the location of the film near a bone-air interface not present in the full body phantom developed by Tino et al. [1].

The results of this study has demonstrated the feasibility of 3D printing a cost-efficient anthropomorphic phantom with realistic geometry and heterogeneities. The resulting custom-made phantom showed similar results to more complex or commercial phantoms for PSQA of SBRT plans, highlighting its potential use for future SBRT commissioning and routine quality assurance purposes. The cost of a full body 3D printed phantom (combining two halves of the body phantom) from this study is approximately $300–400 AUD. This is in contrast to

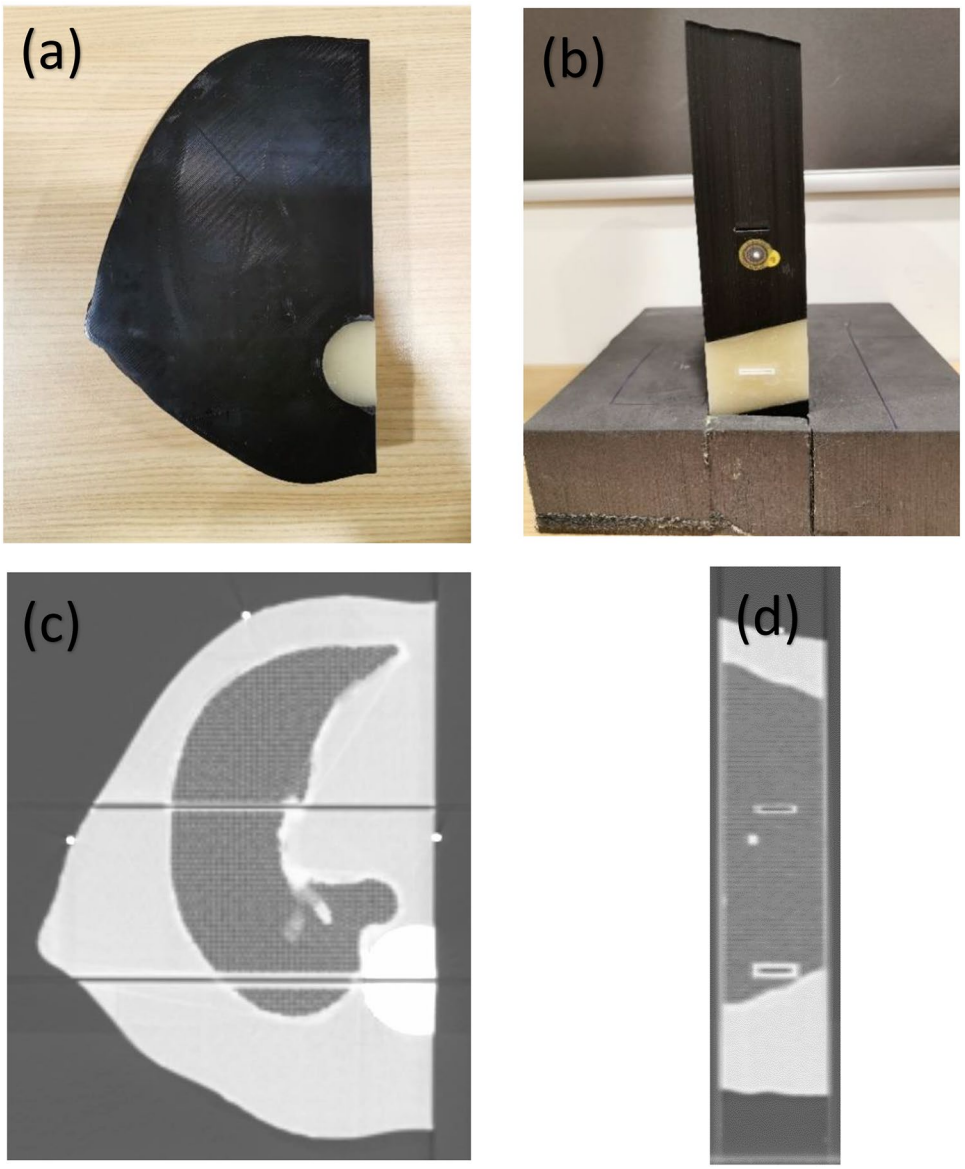

Fig. 4 Images of the anthropomorphic 3D printed phantom **a** axial and **b** sagittal view along with CT scans of the phantom's **c** axial and **d** sagittal view. In the CT scan, the film inserts measuring 15 mm wide and 1 mm in height can be seen placed throughout the phantom

Table 3 Table of the 3D printed anthropomorphic phantom RED_w, mean HU densities, and standard deviation (k = 2) in HU as measured using the same CT scanner and clinical protocol (120 kVp, 2 mm slice thickness)

3DP material substitute	$RED_w(\rho_e/\rho_{e,w})$	Mean CT number (HU)	± SD (HU)
Tissue (PLA 80% zig-zag in-fill)	0.987	− 15	20
Lung (PLA 26% gyroid in-fill)	0.298	− 690	30
Bone (approx. 6% w/w $BaSO_4$)	1.38	650	80

commercial phantoms which can cost thousands of AUD. Furthermore it is simple to design a 3D phantom as the models can come from contours in the structure set which can be further edited using a simple CAD software such as the beginner friendly TinkerCAD (Autodesk, USA). Therefore this study can be reproduced in clinical radiotherapy departments with access to a suitable 3D printer to fabricate an anthropomorphic phantom with equivalent tissue, lung, and bone densities.

Table 4 The gamma passing rates for each criteria as measured by Gafchromic™ EBT3 film inserted into the 3D printed phantom and analysed in SNC Patient

SBRT Plan	5%1 mm (γ) (%)	3%2 mm (γ) (%)
Lung	99.7	95.4
Bone	85.6	84.2

Analysis was performed with 10% low dose threshold and global normalization while 1 mm of the edge of the film was cropped to reduce uncertainty in the results from delamination

Conclusion

This study has shown the feasibility for clinical departments to 3D print substitutes for tissue, lung and bone equivalency that are low cost and readily available. PLA 80% zig-zag in-fill was used for tissue equivalency, PLA 26% gyroid in-fill was used for lung equivalency and a 6% w/w of $BaSO_4$ radio-opacifier was added to an epoxy resin potting mix for bone equivalency. A CT dataset was used to design and fabricate a 3D printed 5 cm thick anthropomorphic thorax slab phantom for SBRT PSQA with realistic geometric and heterogeneity simulation. An end-to end-test was performed with the 3D printed phantom using lung SBRT and bone SBRT plans delivered to Gafchromic™ EBT3 film strips inserted through the phantom.

Gamma analysis was performed in SNC Patient using a 10% low dose threshold, 5%/1 mm and 3%/2 mm gamma criteria. The gamma pass rate across both gamma criteria was ≥ 95% and ~ 85% for lung SBRT and bone SBRT plans respectively. The bone SBRT plan gamma pass rates were lower due to the film being placed at the edge of the phantom where there was a spine-air interface. It is expected that a larger 3D printed phantom joined together from individual 3D printed slabs will allow better agreement for bone SBRT.

This study demonstrates that 3D printers have allowed customisable anthropomorphic phantoms to be fabricated at clinical radiotherapy departments. A phantom similar to the one in this study provides commissioning and quality assurance towards stereotactic type radiotherapy for lesions located in small field heterogeneity. A clinical radiotherapy department using a similar methodology in this study, can manufacture its own customisable anthropomorphic 3D phantoms to meet its own quality assurance needs.

Acknowledgements This study has received support from the Health Education Training Institute Rural Research Capacity Building Program (HETI RRCBP). The author would also like to thank David Schmidt, Kerith Duncanson and Claire Dempsey for their support and contributions throughout the course of this project.

Author contributions SH wrote the initial draft and subsequent editing, contributed to study design, and performed the investigation and analysis. DB & SC provided supervision, assisted in study design, reviewed the manuscript and helped with visualization. GD built the test inserts and post-processed the 3D phantom while AS designed and built the 3D phantom.

Funding This work was supported by the Health Education and Research Institute (HETI) for the Rural Research Capacity Building Program (RRCBP).

Data availability Data available on request from the corresponding author.

Declarations

Competing interests The authors have no relevant conflicts of interest to disclose.

Ethical approval This study has been categorised as a Quality Improvement (QI) project and does not require ethical approval as reviewed by the Greater Western Human Research Ethics Committee (GWHREC).

Consent to participate Written informed consent to use the de-identified CT dataset for academic research purposes was obtained by the department.

Consent to publish Written informed consent to publish not identifiable data was obtained by the department.

References

1. Tino RB, Yeo AU, Brandt M, Leary M, Kron T (2022) A customizable anthropomorphic phantom for dosimetric verification of 3D-printed lung, tissue, and bone density materials. Med Phys 49(1):52–69. https://doi.org/10.1002/mp.15364
2. Kairn T, Zahrani M, Cassim N, Livingstone AG, Charles PH, Crowe SB (2020) Quasi-simultaneous 3D printing of muscle-, lung- and bone-equivalent media: a proof-of-concept study. Phys Eng Sci Med 43(2):701–710. https://doi.org/10.1007/s13246-020-00864-5
3. Ehler ED, Barney BM, Higgins PD, Dusenbery KE (2014) Patient specific 3D printed phantom for IMRT quality assurance. Phys Med Biol 59(19):5763–5773. https://doi.org/10.1088/0031-9155/59/19/5763
4. Leary M et al (2015) Additive manufacture of custom radiation dosimetry phantoms: an automated method compatible with commercial polymer 3D printers. Mater Des 86:487–499. https://doi.org/10.1016/j.matdes.2015.07.052
5. Tino R, Yeo A, Leary M, Brandt M, Kron T (2019) A systematic review on 3D-printed imaging and dosimetry phantoms in radiation therapy. Technol Cancer Res Treat 18:1–14. https://doi.org/10.1177/1533033819870208
6. Goodall SK, Rampant P, Smith W, Waterhouse D, Rowshanfarzad P, Ebert MA (2021) Investigation of the effects of spinal surgical implants on radiotherapy dosimetry: a study of 3D printed phantoms. Med Phys 48(8):4586–4597. https://doi.org/10.1002/mp.15070
7. Ceh J et al (2017) Bismuth infusion of ABS enables additive manufacturing of complex radiological phantoms and shielding equipment. Sensors (Switzerland) 17(3):1–11. https://doi.org/10.3390/s17030459
8. Menzel H-G (2014) International commission on radiation units and measurements. J Int Commun Radiat Units Meas 14(2):1–2. https://doi.org/10.1093/jicru/ndx006

9. Benedict SH et al (2010) Stereotactic body radiation therapy: The report of AAPM Task Group 101. Med Phys 37(8):4078–4101. https://doi.org/10.1118/1.3438081
10. Halvorsen PH et al (2017) AAPM-RSS medical physics practice guideline 9.a. for SRS-SBRT. J Appl Clin Med Phys 18(5):10–21. https://doi.org/10.1002/acm2.12146
11. IAEA (2016) COMMISSIONING OF RADIOTHERAPY TREATMENT PLANNING SYSTEMS: testing for typical external beam treatment techniques. International Atomic Energy Agency
12. Tino R, Leary M, Yeo A, Kyriakou E, Kron T, Brandt M (2020) Additive manufacturing in radiation oncology: a review of clinical practice, emerging trends and research opportunities. Int J Extrem Manuf 2(1):012003. https://doi.org/10.1088/2631-7990/ab70af
13. Kairn T, Peet S, Yu L, Crowe S (2018) Long-term reliability of optically stimulated luminescence dosimeters. World Congr Med Phys Biomed Eng 68(3):561–564. https://doi.org/10.1007/978-981-10-9023-3_103
14. Van der Walt M, Crabtree T, Albantow C (2019) PLA as a suitable 3D printing thermoplastic for use in external beam radiotherapy. Australas Phys Eng Sci Med 42(4):1165–1176. https://doi.org/10.1007/s13246-019-00818-6
15. Hamedani BA, Melvin A, Vaheesan K, Gadani S, Pereira K, Hall AF (2018) Three-dimensional printing CT-derived objects with controllable radiopacity. J Appl Clin Med Phys 19(2):317–328. https://doi.org/10.1002/acm2.12278
16. Tino R, Leary M, Yeo A, Brandt M, Kron T (2019) Gyroid structures for 3D-printed heterogeneous radiotherapy phantoms. Phys Med Biol 64(21):21NT05. https://doi.org/10.1088/1361-6560/ab48ab
17. Zavan R, McGeachy P, Madamesila J, Villarreal-Barajas JE, Khan R (2018) Verification of Acuros XB dose algorithm using 3D printed low-density phantoms for clinical photon beams. J Appl Clin Med Phys 19(3):32–43. https://doi.org/10.1002/acm2.12299
18. Markwell T, Sim L, Zawlodzka S (2020) Can 3D printed phantoms accurately model low-density lung? Investigating the accuracy of Pinnacle for low density lung calculations using 3D printed phantoms
19. Ehler E, Craft D, Rong Y (2018) 3D printing technology will eventually eliminate the need of purchasing commercial phantoms for clinical medical physics QA procedures. J Appl Clin Med Phys 19(4):8–12. https://doi.org/10.1002/acm2.12392
20. Okkalidis N, Marinakis G (2020) Technical note: accurate replication of soft and bone tissues with 3D printing. Med Phys 47(5):2206–2211. https://doi.org/10.1002/mp.14100
21. Crowe SB et al (2020) Impact of radiopacified bone cement on radiotherapy dose calculation. Phys Imaging Radiat Oncol 14:12–16. https://doi.org/10.1016/j.phro.2020.04.004
22. Dancewicz OL, Sylvander SR, Markwell TS, Crowe SB, Trapp JV (2017) Radiological properties of 3D printed materials in kilovoltage and megavoltage photon beams. Phys Medica 38:111–118. https://doi.org/10.1016/j.ejmp.2017.05.051
23. Australian Government: National Health and Medical Research Council (2018) Conduct in human research national statement on ethical conduct in human research. 2007
24. Lewis D, Micke A, Yu X, Chan MF (2012) An efficient protocol for radiochromic film dosimetry combining calibration and measurement in a single scan. Med Phys 39(10):6339–6350. https://doi.org/10.1118/1.4754797